Published in final edited form as:
Dev Biol. 2006 August 15; 296(2): 363–374.

Tgfbr2 regulates the maintenance of boundaries in the axial skeleton

Michael O. Baffi, **Molly A. Moran**, and **Rosa Serra***
Department of Cell Biology, University of Alabama at Birmingham, 1918 University Blvd, 310 MCLM, Birmingham, AL 35294-0005, USA

Abstract

Previously, we showed that deletion of the TGF-β type II receptor (*Tgfbr2*) in Type II Collagen (Col2a) expressing cells results in defects in the development of the axial skeleton. Defects included a reduction in size and alterations in the shape of specific vertebral elements. Anterior lateral and dorsal elements of the vertebrae were missing or irregularly shaped. Vertebral bodies were only mildly affected, but the intervertebral disc (IVD) was reduced or missing. In this manuscript, we show that alterations in the initiation or proliferation of cartilage are not detected in the axial skeleton. However, the expression domain of Fibromodulin (Fmod), a marker of the IVD, was reduced and the area of the future IVD contained peanut agglutinin (PNA) staining cartilage. Next, we show that the expression domains of Pax1 and Pax9, which are preferentially expressed in the caudal sclerotome, are expanded over the entire rostral to caudal length of the sclerotome segment. Dorsal–ventral patterning was not affected in these mice as accessed by expression of Pax1, Pax9, and Msx1. Proliferation was modestly reduced in the loose cells of the sclerotome. The results suggest that signaling through Tgfbr2 regulates the maintenance of boundaries in the sclerotome and developing axial skeleton.

Keywords

TGF-β; Axial skeleton; Sclerotome; Pax

Introduction

Somitogenesis establishes the metamerism that is a defining feature of all vertebrates. The somites bud off of the paraxial or presomitic mesoderm in a pairwise manner bilateral to the axial notochord and neural tube (reviewed in Christ et al., 2004; Stockdale et al., 2000). Prior to overt morphological segmentation, the presomitic mesoderm undergoes a rostral–caudal polarization on a molecular level defining the prospective somite (Saga and Takeda, 2001). Once formed, the somites are comprised of an epithelial sphere containing a mesenchymal core, the somitocoel. The subsequent maturation process of the somites along the anterior–posterior axis generates the components that define the axial skeleton. This maturation is facilitated by signals that are derived from the notochord, neural tube, ectoderm and lateral plate mesoderm. The first indication of differentiation occurring is marked by the epithelial to mesenchymal transition of the ventromedial half of the somite. This transition generates the sclerotome, which includes the former somitocoel.

The sclerotome will establish the vertebral anlagen through the orchestration of its dorsal, lateral, and ventral populations. The dorsal sclerotome expresses Msx1, which is induced by

*Corresponding author. Fax: +1 205 975 5648. *E-mail address:* rserra@uab.edu (R. Serra)..

BMP-4 secreted from the roof plate and ectoderm, and later forms the dorsal part of the neural arch and the spinous process (Monsoro-Burq, 2005; Monsoro-Burq et al., 1994, 1996). The development of the lateral sclerotome depends on signals from the notochord and myotome (Henderson et al., 1999). This sclerotome population will form the laminae and pedicles of the neural arches and the ribs. Ventral sclerotome is made up of Pax1 and Pax9 expressing cells that have invaded the perinotochordal space and will give rise to the vertebral bodies and IVD (Balling et al., 1996; Peters et al., 1999). Along the rostral–caudal axis, the sclerotome is segmented into regions of loose and condensed mesenchyme, respectively. This morphological polarization of the scler-otome is also apparent on the molecular level through the differential expression of such genes as Tbx18 in the rostral sclerotome and Pax1 and Pax9 in the caudal domain (Bussen et al., 2004; Kraus et al., 2001; Peters et al., 1999; Walin et al., 1994). Due to the process of resegmentation, the IVD forms from condensed mesenchyme derived from the somitocoel at the border of the rostral and caudal domains (Huang et al., 1996, 2000; Mittapalli et al., 2005; Stern and Vasiliauskas, 2000). Then the rostral sclerotome will form the caudal portions of the mature vertebrae while the caudal sclerotome will form the rostral portions of the vertebrae. As chondrogenesis proceeds, the notochord cells are removed from the vertebral region and expand into the IVD region to form the embryonic nucleus pulposus (Paavola et al., 1980). The nucleus pulposus is surrounded by the annulus fibrosus, which is derived from sclerotome (Rufai et al., 1995).

Previously, we reported multiple defects in the axial skeleton of mice in which *Tgfbr2* was deleted in Col2a expressing cells using the Cre/lox recombinase system (Baffi et al., 2004). Mice expressing Cre under the control of the *Col2a* promoter (Col2a-Cre; Ovchinnikov et al., 2000) were crossed to mice in which the *Tgfbr2* gene was flanked with bacterial LoxP sites (Chytil et al., 2002). The expression pattern of Cre in the Col2a-Cre mice was shown previously using the ROSA 26-Cre reporter mouse strain (Ovchinnikov et al., 2000). Cre activity was first detected at E9.5 days in the sclerotome. Cre expression continued at E12.5 days in the vertebral anlagen. Low levels of expression were also detected in the notochord. By E15 days, activity was seen in the entire cartilage model of both the appendicular and axial skeleton (Baffi et al., 2004; Ovchinnikov et al., 2000). The phenotype of Col2acre$^{+/-}$; *Tgfbr*$^{loxP/loxP}$ mice included a reduction in size and alterations in the shape of the vertebrae. Anterior lateral and dorsal elements of the vertebrae were missing or irregularly shaped. The size and shape of vertebral bodies in E17.5-day embryos were mildly affected but IVD was greatly reduced or missing (Baffi et al., 2004). In this study, we address the mechanism of some of the observed phenotypes. Alterations in the initiation or proliferation of vertebral chondrocytes were not detected; however, a modest reduction in the proliferation of sclerotome was observed. A defect in the maintenance of the boundary between the presumptive IVD and vertebrae was observed. In addition, expansion of the rostral–caudal domain of Pax 1 and Pax 9 expression with no associated defect along the dorsal–ventral axis was detected. We propose that one of the functions of Tgfbr2 in the developing axial skeleton is to maintain boundaries between cell types.

Materials and methods

Identification of transgenic mice

For timed pregnancies, specific matings were set-up in the afternoon, and the mice were checked for vaginal plugs the next morning. Noon on the day of the vaginal plug was considered 0.5 days of gestation. The genotype of transgenic mice was determined by PCR analysis of genomic DNA isolated from mouse tails by proteinase K digestion and phenol/chloroform extraction. Col2a-Cre mice were obtained from Jackson Laboratories (Bar Harbor, Maine; Ovchinnikov et al., 2000). PCR for the Cre transgene was performed using the following primers: Cre forward (5′ TGC TCT GTC CGT TTG CCG3′) and Cre reverse (5′ ACT GTG

TCC AGA CCA GGC3′). Genomic DNA was amplified for 34 cycles of denaturation at 94° C for 30 s, annealing at 58°C for 60 s, and elongation for 90 s at 72°C in reaction buffer containing 2.5 mM $MgCl_2$, 1× PCR buffer (HotMaster Taq buffer, Eppendorf), 0.2 mM dNTPs (Pharmacia, Uppsala, Sweden), 0.2 μM each primer. *Tgfbr2*-loxP mice were obtained from Dr. H.L. Moses, Vanderbilt University, Nashville, TN (Chytil et al., 2002). The loxP allele was identified using the following primers: lox1forward (5′ TAA ACA AGG TCC GGA GCC CA3′) and lox1 reverse (5′ ACT TCT GCA AGA GGT CCC CT3′). Two bands can be detected with these primers. One band represents the wild-type allele (420 bp) and another represents the loxP allele (540 bp).

Peanut agglutinin (PNA) staining

Embryos were genotyped, fixed in 4% cold paraformaldehyde, embedded in paraffin, and sectioned. Sections were dewaxed in xylene followed by rehydration in an ethanol series. Slides were washed in PBS then incubated with 10 μg/ml rhodamine conjugated PNA (Vector Laboratories) for 2 h at room temperature. The slides were washed and counterstained with YoPro (Molecular Probes). Images were captured using an Olympus BX51microscope and Macrofire digital camera.

In situ hybridization

Radioactive in situ hybridization (RISH) was performed as described (Pelton et al., 1990) on sections from mouse embryos. Sections were hybridized to ^{35}S-UTP labeled sense and antisense riboprobes. Images of the sections were obtained using an Olympus BX51 microscope and Macrofire digital camera. Images were taken under bright field and dark field illumination. In some cases, pseudo-colored dark field and bright field images were merged.

Whole-mount in situ hybridization (WISH) was performed as described (Wilkinson and Nieto, 1993) on whole mouse embryos. Embryos were hybridized to digoxigenin (DIG)-UTP labeled antisense riboprobes. Hybridization was detected with an alkaline phosphatase-conjugated anti-DIG antibody and NBT/BCP or BM purple substrate. Images were taken using an Olympus SZX12 dissecting microscope and Magnafire digital camera.

Probes for in situ hybridization were generated by RT-PCR and subcloned into the pGEM-T Easy (Promega) cloning vector. The primers and resulting size of each fragment are as follows: Msx1, 494 bp, forward: 5′ GAGTCCTTCCTAGGAAGCTC, reverse: 5′ AACCTACCTTGGTGAAGCAGC; Sox9, 333 bp, forward: 5′ GAGAAAAGCTATGGTGACAGAGC, reverse: 5′ GTC CTCCATGTTAACTCT-GAAGG; Fibromodulin, 585 bp, forward: 5′ ATGAACTTCTCCAAGCT GCAGG; reverse: CCTAAGACATTAGAAGAGGCCC; Tbx18, 429, forward: 5′ GCGTTGG AATCTAGTGGATC; reverse: 5′ GAGATCGCAAGGCTATCAAC. All inserts were sequence verified. Probes for Pax1 and Pax 9 were a kind gift from Dr. B. Wilm and Dr. R. Balling Institute of Mammalian Genetics, Germany (Peters et al., 1999).

Proliferation assays

For detection of proliferating cells, pregnant dames were injected with 0.06 g BrdU/g mouse 2.5 h before sacrifice and removal of the embryos. The embryos were genotyped, fixed, embedded, and sectioned. BrdU-stained nuclei were identified by immunofluorescent staining as previously described (Baffi et al., 2004). In some cases, as indicated, Ki67 (AB-4; NeoMarker #rb-1510-po) or Cyclin D3 (Cell Signaling Technologies, #9932) staining was used to identify proliferating cells. Antigen retrieval was accomplished by heating sections in sodium citrate buffer (10 mM sodium citrate, pH to 6.0, 0.05% Tween 20) for 20 min at 95° C. Sections were counterstained with YoPro (Molecular Probes), a green nuclear stain. Fluorescence was observed and imaged using an Olympus BX-51 upright microscope with a

Magnafire digital camera. The percent labeled nuclei was determined by counting red/red + green nuclei in cartilage (perichondrium, IVD, etc. was excluded) from four to eight microscope fields from several mice of each genotype, Cre−; *Tgfbr2*$^{+/lox}$ and Cre+; *Tgfbr2*$^{lox/lox}$, pooled from several litters. Since the numbers between litters at each stage were not statistically different, we chose to pool the data within each stage for further statistical analysis. The mean and standard deviation were calculated, and significant differences between each group were determined using a Student's *T* test. Results that were statistically different were determined by a P value <0.05.

Results

Loss of Tgfbr2 results in reduced proliferation in the loose cells of the sclerotome but does not affect initiation or proliferation of chondrocytes

We previously showed that conditional deletion of *Tgfbr2* in Col2a expressing cells resulted in defects in the development of the axial skeleton including a decrease in the overall size of the vertebral elements. We hypothesized that this could be due to a defect in endochondral bone formation within the sclerotome. Endochondral bone formation is the process by which a cartilage template pre-forms the skeletal element that is subsequently replaced with bone (Cancedda et al., 1995; DeLise et al., 2000). In the vertebrae, chondrogenesis occurs in the sclerotome after it is formed and patterned. Cells within the sclerotome move through a progressive series of differentiation steps establishing proliferating, prehypertrophic and hypertrophic subpopu-lations. One of the earliest markers of chondrogenesis is the HMG-box transcription factor Sox9. Sox9 expression was detected by radioactive in situ hybridization on sagittal sections of E12.5-day embryos (Figs. 1A, B). Along the entire length of the developing vertebral column, the Sox9 expression pattern was comparable in both control and Col2acre$^{+/-}$;*Tgfbr*$^{loxP/loxP}$ experimental mice. The comparable expression pattern of Sox9 expression suggests that there is no defect in the initiation of chondrogenesis in the absence of Tgfbr2.

It is also possible that the reduced size of the vertebrae is a result of altered proliferation in chondrocytes after they differentiate from sclerotome. To test this possibility, we measured the percentage of nuclei that labeled with BrdU in vertebral chondrocytes from E14.5- and E12.5-day embryos (Table 1). Pregnant dams were injected intraperitoneal with 10 μM BrdU 2.5 h before being sacrificed. E12.5 and E14.5 embryos were collected and genotyped using DNA isolated from extraembryonic tissue. Next, embryos were fixed and embedded in paraffin and cut into serial transverse or sagittal sections. Immunostaining was performed using a rat mAb directed to BrdU, a biotinylated secondary antibody, and Cy3-conjugated avidin (red). Sections were counterstained with Yo Pro (green). The percent labeled nuclei was determined by counting red/red + green nuclei in histological defined cartilage. Perichondrium, IVD and other tissues were excluded. Four to eight microscope fields from four E14.5-day mice of each genotype, Cre−; *Tgfbr2*$^{+/lox}$ and Cre+; *Tgfbr2*$^{lox/lox}$, pooled from three litters were counted. Labeled cells in sections from two E12.5-day mice of each genotype were also counted. Since the numbers between litters at each stage were not statistically different, we chose to pool the data within each stage for further statistical analysis. Differences in chondrocyte proliferation in the axial skeleton were not observed between Cre-negative and Cre+; *Tgfbr2*$^{lox/lox}$ mice. The data suggest that the vertebral phenotype observed in Cre+; *Tgfbr2*$^{lox/lox}$ mice is not due to reduced proliferation of chondrocytes and that once the cartilage forms, it proliferates normally. We previously showed that hypertrophic differentiation was not altered in the axial or appendicular skeleton of the Cre+; *Tgfbr2*$^{lox/lox}$ mice (Baffi et al., 2004). Together the data suggest Tgfbr2 is not required for normal endochondral bone formation in the axial skeleton and suggest that some of the phenotype observed in these mice could be a result of alterations in the sclerotome that precede chondrogenesis.

Since Cre is expressed in the sclerotome at E9.5 days, before overt chondrogenesis, conditional deletion of *Tgfbr2* may alter proliferation and expansion of the sclerotome cells, which would result in fewer cells available for chondrogenesis and smaller vertebral elements. Since the development of the sclerotome and vertebral chondrogenesis starts in the anterior of the mouse and moves posterior, it is possible to analyze several stages of sclerotome in the E12.5-day embryo. While clear areas of cartilage are observed in the cervical and thoracic regions of the mouse at this stage, the tail contains undifferentiated sclerotome that is divided into rostral and caudal domains defined by loose and condensed mesenchyme respectively. IVD will form from most of the condensed sclerotome, and the vertebrae will form primarily from the loose cells. We compared the level of proliferation in the sclerotome of the tail region in Cre− controls and Cre+; *Tgfbr2*$^{lox/lox}$ embryos using both BrdU incorporation as described above and staining for Cyclin D3 expression (Table 1). Both methods gave similar results. A small but statistically significant decrease in proliferation was detected in the loose mesenchyme of the sclerotome while proliferation in the condensed area was similar in Cre-negative and Cre+; *Tgfbr2*$^{lox/lox}$ mice. The results suggest that at least part of the phenotype observed in the Cre+; *Tgfbr2*$^{lox/lox}$ mice is due to defects in proliferation of the sclerotome perhaps leading to fewer cells available for the subsequent development of the vertebrae.

Tgfbr2 is required for the maintenance of the boundaries in the sclerotome

IVD is composed of two principle components, the nucleus pulposus, initially derived from the notochord, and the region surrounding the nucleus pulposus, the annulus fibrosus, derived from the sclerotome. We had previously shown that IVD is reduced or absent in mice with the *Tgfbr2* conditional deletion (Baffi et al., 2004). To assess the development of the IVD, we examined the histology of the developing IVD and the expression of the proteoglycan Fibromodulin (Fmod) by radioactive in situ hybridization (Fig. 2). Fmod is preferentially expressed in IVD (Smits and Lefebvre, 2003). Alterations in the inner annulus were detected in hematoxylin and eosin (H&E) stained sagittal sections from E14.5 day Col2acre$^{+/-}$;*Tgfbr2*$^{loxP/loxP}$ mice when compared to sections from control littermates (Figs. 2A, B). In sections from control embryos, a clear demarcation between the condensed spindle cells of the IVD region and the area of chondrogenesis in the vertebral body was observed. Cells in the control IVD were spindle shaped and arranged into a concentric pattern around the nucleus pulposus (Fig. 2A inset). In the sections from Col2acre$^{+/-}$; *Tgfbr2*$^{loxP/loxP}$ mice, cells within the annulus fibrosus were not well organized and had a round morphology (Fig. 2B inset). In addition, the nucleus pulposus was often shifted dorsally within the IVD. Alterations in the annulus fibrosus were confirmed by the expression pattern of Fmod as determined by radioactive in situ hybridization to sagittal and transverse sections from E14.5-day embryos (Figs. 2C–F). Fmod expression was localized primarily to the annulus fibrosus in the control mice (Figs. 2C, E). Whereas the expression of Fmod was virtually lost in the Col2acre$^{+/-}$;*Tgfbr*$^{loxP/loxP}$ experimental mice (Figs. 2D, F). Fmod expression in the lung was comparable in Cre+ and Cre− mice indicating the specificity of the effect (not shown). The reduced expression of Fmod in the Col2acre$^{+/-}$; *Tgfbr*$^{loxP/loxP}$ experimental mice in the presumptive IVD suggests a potential defect in the specification or maintenance of the cells of the annulus fibrosus.

To determine if the cells of the IVD were replaced with cells with more cartilage character, we compared the pattern of staining with peanut agglutinin (PNA) in Col2acre− and Col2acre$^{+/-}$;*Tgfbr*$^{loxP/loxP}$ embryos (Figs. 3 and 4). PNA is a lectin that recognizes β -galactose (1–3) *N*-acetyl galactosamine residues. It is commonly used to detect chondrogenic tissues and can detect chondrogenic cells before the overt deposition of cartilage specific matrix and staining with Alcian blue (Bagnall and Sanders, 1989;Delise and Tuan, 2002;Stringa and Tuan, 1996). First, sections from E14.5-day embryos were stained with rhodamine conjugated PNA (red) followed by counter-staining with a green nuclear stain, YoPro (Fig. 3). In control

embryos, PNA staining was observed in the developing thoracic vertebrae with almost no staining detected in the future IVD (Fig. 3A). There was a sharp demarcation in the staining between these two areas suggesting a strong border between cells that will form the vertebrae and those that will form the IVD. In the cervical region, where the development of the axial skeleton is more advanced, there was a low level of staining in the ventral region of the annulus fibrosus but there was still a clear demarcation between the vertebrae and the IVD (Fig. 3C). Staining was also observed in the nucleus pulposus and sheath of the remaining notochord. In contrast, a clear demarcation in PNA staining between the vertebrae and IVD areas was not observed in sections from thoracic and cervical vertebrae of Col2acre$^{+/-}$;*Tgfbr*$^{loxP/loxP}$ embryos (Figs. 3B, D). In the thoracic region, staining in the vertebrae was uneven and was slightly higher on the caudal side. In the cervical region, high levels of staining we detected on both the ventral and dorsal aspects of the presumptive IVD suggesting these cells had chondrogenic character. Staining in the nucleus pulposus was similar to control mice. The results suggest that Tgfbr2 regulates the boundary between the IVD and vertebrae, perhaps by preventing chondrogenic differentiation in the cells of the annulus fibrosus.

Alterations in the boundary between the future vertebrae and future IVD could be detected in the cervical, thoracic, and upper lumbar regions as early as E12.5 days (Fig. 4). Repeating segments containing three distinct cell populations could be seen in H&E stained and PNA stained sections from E12.5-day control embryos (Figs. 4A (H&E), C, E (PNA merged)). In H&E stained sections, the dark staining condensed area that represents the future IVD area was designated as domain 1 (Fig. 4A). This area was devoid of PNA staining and had the highest density of nuclear (green) staining (Figs. 4C, E). Domain 2 was directly caudal to domain 1 and contained chondrogenic cells as determined by the expression of PNA (Figs. 4A, C, E). PNA staining was more intense on the caudal half of domain 2 although light and diffuse staining was observed in the rostral half of domain 2. Domain 3 consisted of a very thin stripe of cells separating the caudal part of domain 2 from the rostral part of domain 1 (Fig. 4A inset). This small stripe of cells had no PNA staining and few nuclei providing a strong break in PNA staining between the developing vertebrae and IVD (Figs. 4C, E merged). In contrast, domain 3 was not detectable in sections from Col2acre$^{+/-}$;*Tgfbr*$^{loxP/loxP}$ embryos (Figs. 4B (H&E), D, F (PNA merged)). As a result, there was not a strong boundary between PNA staining in the caudal half of domain 2 and domain 1(Figs. 4B inset and C–F red channel). In the cervical region of Col2acre$^{+/-}$;*Tgfbr*$^{loxP/loxP}$ embryos, PNA stained cells could be seen invading domain 1 (Figs. 4E, F). The results suggest Tgfbr2 is required to maintain the boundaries between different compartments of the axial skeleton as early as E12.5 days.

Loss of Tgfbr2 alters the rostral–caudal boundary of the sclerotome but does not affect dorsal–ventral patterning

Since defects in the dorsal aspects of the vertebrae were previously reported in Col2acre$^{+/-}$;*Tgfbr*$^{loxP/loxP}$ mice, we tested the hypothesis that deletion of *Tgfbr2* would affect dorsal ventral patterning in the sclerotome. The dorsal sclerotome expresses Msx1, which is induced by BMP-4 secreted from the roof plate and ectoderm, and later forms the dorsal part of the neural arch and the spinous process (Monsoro-Burq et al., 1994, 1996). The paired box containing transcription factors Pax1 and Pax9 is expressed in the ventral domain of the sclerotome (Peters et al., 1995, 1999). First, whole-mount and radioactive in situ hybridization of Msx1 and Pax9 in E11.5 and E12.5-day embryos was used to localize and determine the presence and establishment of the dorsal and ventral sclerotome. Pax 9 shared a common expression pattern between control and Col2acre$^{+/-}$;*Tgfbr*$^{loxP/loxP}$ mice (Figs. 5A, B). The expression was localized in the ventral sclerotome surrounding the notochord and expanded lateral and dorsal to approximately the same extent in control and experimental embryos. Msx1 was also expressed in a comparable domain in the control and Col2acre$^{+/-}$;*Tgfbr*$^{loxP/loxP}$ E11.5- and E12.5-day embryos (Figs. 5B–D). The expression was focused most dorsally in the region

between the roof plate of the neural tube and the surface ectoderm. The proper localization of both Msx1 and Pax9 in the dorsal and ventral domains of the sclerotome respectively indicates that the dorsal–ventral specification of the sclerotome was not interrupted by the deletion of *Tgfbr2*.

We had also reported defects in the formation of the lateral aspects of the vertebrae including the absence of specific anterior lateral structures (Baffi et al., 2004). We hypothesized that this defect could be due to alteration in the rostral–caudal polarity of the sclerotome segment. To test this hypothesis, the rostral–caudal expression domains of Pax1 and Pax9 were determined by whole-mount in situ hybridization and compared in control and Col2acre$^{+/-}$;*Tgfbr*$^{loxP/loxP}$ E11.5-day embryos (Fig. 6). The expression of Pax1 precedes that of Pax9 and is initially found in all sclerotome cells. At later stages of sclerotome differentiation, the expression of Pax1 acquires a maximum in the caudal, ventromedial domain, whereas the expression of Pax9 is found in the caudal, ventrolateral domain (Peters et al., 1995, 1999; Walin et al., 1994). Here, Pax1 and Pax9 mRNA were preferentially localized to the caudal half of the sclerotome in the lumbar and tail regions of E11.5-day control embryos (Figs. 6A, C). In contrast, the expression domain of Pax1 and Pax9 was expanded rostrally, encompassing the entire sclerotome segment in Col2acre$^{+/-}$;*Tgfbr*$^{loxP/loxP}$ embryos (Figs. 6B, D) The result suggests that Tgfbr2 normally restricts the expression domain of Pax1 and Pax9 to the caudal half of the sclerotome. It also suggests that Tgfbr2 could regulate rostral–caudal polarity within the sclerotome.

The expression of the T-box transcription factor Tbx18 is confined to the rostral sclerotome and has been used as a marker for cells with rostral character (Bussen et al., 2004; Kraus et al., 2001). In addition, neural crest cells are inhibited from migrating across the posterior portion of the sclerotome (Bronner-Fraser, 1993). Axons from the dorsal root ganglion and motor neurons pass only through the anterior portion of each sclerotome and avoid migrating through the posterior regions. The rostral domain of the sclerotome is caudalized in mice with targeted deletion of the *Tbx18* gene (Bussen et al., 2004). That is, the dorsal root ganglion is not segmented normally, and the expression domain of Pax9 is expanded. Since the expression domain of Pax1 and Pax 9 was expanded in Col2acre$^{+/-}$;*Tgfbr*$^{loxP/loxP}$ embryos, we next tested the hypothesis that the rostral character of the sclerotome was lost and replaced with cells of caudal character. We first looked at the organization of the dorsal root ganglion and the developing vertebrae (Figs. 7A, B). In E12.5-day embryos, the dorsal root ganglion and the associated motor axons appeared to be segmented and organized in both control and experimental embryos indicating that the rostral half of the sclerotome did not express the inhibitory activity of the caudal sclerotome. Next, expression of Tbx18 was compared in control and Col2acre$^{+/-}$; *Tgfbr*$^{loxP/loxP}$ embryos by radioactive in situ hybridization (Figs. 7C, D). The Tbx18 expression domain was segmented and localized in the rostral sclerotome in both control and Col2acre$^{+/-}$;*Tgfbr*$^{loxP/loxP}$ embryos (Figs. 7C, D). Likewise, Tbx18 mRNA was restricted to the rostral domain of the sclerotome in E10.5- and E11.5-day control and experimental embryos as determined by whole-mount in situ hybridization (not shown). The results suggest that loss of *Tgfbr2* does not caudalize the sclerotome; however, Tgfbr2 is involved in regulating the expression boundaries for Pax1 and Pax9.

Discussion

The results presented here provide information regarding the role of Tgfbr2 in development of the axial skeleton. The similar expression of Sox9 in the presumptive vertebrae of control and experimental mice suggest that Tgfbr2 is not required for the initiation of chondrogenesis. Alterations in chondrocyte proliferation were not detected in mice with targeted deletion of *Tgfbr2*; however, a modest decrease in proliferation was detected in the loose cells of the sclerotome. The results suggest that once chondrogenesis starts, it proceeds normally but there

may be fewer cells initially available resulting in smaller vertebrae. In addition, the loss of Fmod expression in the presumptive IVD in experimental mice suggested a potential defect in the specification or maintenance of the disc cells. PNA stained cartilage was observed in the IVD space at E14.5 days, and the boundaries between vertebrae and IVD were blurred as early as E12.5 days suggesting Tgfbr2 is required to maintain the boundary between the developing vertebrae and IVD. For the purposes of understanding the role of Tgfbr2 on the patterning of the dorsal and ventral sclerotome, a selection of morphogenetic markers was used. The ventral sclerotome markers, Pax1 and Pax9, and the dorsal sclerotome marker, Msx1, did not show any differences in their dorsal or ventral expression boundaries between control and experimental mice suggesting that Tgfbr2 is not required for normal dorsal–ventral patterning of the sclerotome. This result led to the assessment of markers that delineate the rostral and caudal domains of the sclerotome. Tgfbr2 regulates the rostral expression boundary of Pax1 and Pax9 without affecting the segmentation of the dorsal root ganglion or expression of Tbx18 in the rostral domain. Together, the results suggest that Tgfbr2 is required to maintain specific boundaries in the axial skeleton.

We had previously shown that IVD is reduced or absent in mice with the *Tgfbr2* conditional deletion (Baffi et al., 2004). IVD is derived from sclerotome and notochord (Paavola et al., 1980; Rufai et al., 1995; Theiler, 1988). The nucleus pulposus is initially derived from the notochord and the region surrounding the nucleus pulposus, the annulus fibrosus, is derived from the sclerotome. As the vertebral bodies undergo chondrogenesis, notochord cells are removed from the vertebral region and expand into the IVD region to form the nucleus pulposus. The nucleus pulposus of the mature IVD is like cartilage and contains Col2 (Poole, 1998). The annulus fibrosus has properties of both hyaline and fibrous cartilage and provides the structural properties of the IVD. Fmod is preferentially expressed in the developing annulus fibrosus relative to cartilage (Smits and Lefebvre, 2003). In sections from Col2acre$^{+/-}$;*Tgfbr2*$^{loxP/loxP}$ mice, the boundary between the IVD and vertebral body was not clearly demarcated as it was in control mice. The cells in the IVD were round instead of spindle shaped while the notochord and nucleus pulposus appeared normal. Fmod expression was greatly reduced and PNA stained chondrogenic cells were found in the IVD of Col2acre$^{+/-}$; *Tgfbr*$^{loxP/loxP}$ mice relative to Col2acre$^{-/-}$;*Tgfbr*$^{+/loxP}$ controls suggesting that Tgfbr2 is required for the formation or maintenance of the annulus fibrosus cells. Previously, we showed dominant-negative interference of the TGFβ type II receptor (DNIIR) in mice results in osteoarthritis of the peripheral joints (Serra et al., 1997). Although most of the cartilage model will turn to bone, articular cartilage is normally protected and a sharp demarcation between cartilage and bone is maintained in the presence of TGF-β signaling. DNIIR mice and other mice with alterations in the TGF-β signaling pathway demonstrate a similar oseoarthritic phenotype that most likely results from inappropriate hypertrophic differentiation in the articular cartilage (Dabovic et al., 2002; Serra et al., 1997; Yang et al., 2001; Zuscik et al., 2004). Fusion of vertebrae and cartilage metaplasia in the IVD and spinal ligaments were also seen in the DNIIR mice (Serra et al., 1997 and data not shown). Interestingly, polymorphisms within the human *Tgfb1* gene have a weak but significant association with ankylosing spondylitis (Jaakkola et al., 2004), and the T29 to C polymorphism in the *Tgfb1* gene is associated with the genetic susceptibility to spinal osteophytosis (Yamada et al., 2000). Both disorders are characterized by inappropriate chondrogen-esis in the IVD and ligaments followed by fusion of the vertebrae. We propose that Tgfbr2 acts to prevent inappropriate cartilage differentiation in the IVD and that in the absence of Tgfbr2 the boundary between the IVD and vertebrae is lost and cartilage differentiation spreads from the ossification center of the vertebrae into the area of the IVD.

Intrasegment boundaries within the sclerotome are evident histologically and molecularly. Restricted staining with PNA and expression patterns of genes like Pax9 and Tbx18 provides examples of the segmentation within each sclerotome unit. In addition, these segments can be

defined and maintained by intracellular communication and adhesion between cells within each subsegment (Bagnall et al., 1992; Stern et al., 1986; Tam and Trainor, 1994). When fluorescent dye is injected into a cell in the rostral domain, it spreads throughout this domain but not to the central or caudal domain (Bagnall et al., 1992). Similar results are obtained if a cell in the central or caudal domain are injected suggesting direct communication between cells within each subsegment. Furthermore, if cells from the rostral and caudal domains are marked, isolated, and combined in culture, they will separate and form clusters of like cells suggesting the importance of the adhesive properties of the cells in maintaining the boundaries of the subsegments (Stern et al., 1986). It will be interesting to determine if Tgfbr2 regulates these properties in the sclerotome.

The observed defects in the vertebrae and IVD could also be the result of alterations in the maintenance of rostral–caudal polarity, defects in intrasegment boundaries, or resegmentation. The polarity of the sclerotome is determined in the presomitic mesoderm as the somites first develop (Bronner-Fraser and Stern, 1991; Christ et al., 2004). It has been shown that the transcription factors Tbx18 and Uncx4.1 are required for the maintenance of polarity in the sclerotome (Bussen et al., 2004; Leitges et al., 2000; Mansouri et al., 2000). Tbx-18 expression is normally restricted to the rostral domain. Targeted deletion of Tbx18 results in expansion of caudal character at the expense of cells with rostral character leading to an expansion of the Pax9 expression domain, failure of proper segmentation of the dorsal root ganglion, and ultimately expansion and fusion of the lateral vertebrae (Bussen et al., 2004). In contrast, Col2acre$^{+/-}$;*Tgfbr*$^{loxP/loxP}$ embryos have thin vertebrae and are missing anterior lateral structures and IVD suggesting the loss of caudal character, not expansion of one domain at the expense of the other. Suprisingly, we found that the expression domains of Pax1 and Pax9 were expanded rostrally while Tbx18 expression remained restricted to the rostral domain. In addition, segmentation of the dorsal root ganglion appeared normal suggesting the rostral domain was not “caudalized” despite expanded expression of Pax1 and Pax9.

Mice lacking both Pax 1 and Pax 9 do not have vertebral bodies or IVD suggesting an important role for Pax genes in the development of the ventral vertebrae (Peters et al., 1999). Since the entire ventral sclerotome is severely affected in these mice, it is difficult to determine if Pax1 or Pax9 has specific functions in regulating development of rostral and caudal structures; however, it was recently suggested that mutations in human *PAX1* are associated with Klippel-Feil syndrome, which is characterized by scoliosis and fusions in the cervical vertebrae as a consequence of defects in resegmentation (McGaughran et al., 2003; Tracy et al., 2004). The details of resegmentation in the mouse sclerotome are still controversial (Christ et al., 2000; Goldstein and Kalcheim, 1992; Huang et al., 2000). Only a few mouse models have been described as having defects in resegmenta-tion (Johnson et al., 2001; Sporle and Schughart, 1998). Some of the defects observed in the Col2acre$^{+/-}$;*Tgfbr*$^{loxP/loxP}$ mice including split lamina, disorganized costal joints, loss of the IVD, and defects in the anterior articular process would be consistent with defects in resegmentation. Furthermore, a specific joint forming compartment of the sclerotome, the arthrotome, was recently identified (Mittapalli et al., 2005). This compartment is formed from the descendents of the somitocoel cells. Somitocoel cells are the loose mesenchyme located in the center of the epithelial somite. When the sclerotome forms, they make up a portion of the caudal sclerotome near the rostral–caudal border. Removal of these cells results in the loss of IVD and fusion of the anterior and posterior articular processes. It is not known if the deletion of *Tgfbr2* affects the fate of somitocoel cells.

In summary, the results presented here suggest that Tgfbr2 is required to maintain the boundary between the vertebrae and IVD and the rostral expression boundary of Pax1 and Pax9 in the sclerotome. Failure to maintain the subsegments within the axial skeleton likely contributes to the phenotypes observed in the Col2acre$^{+/-}$;*Tgfbr*$^{loxP/loxP}$ mice. Future experiments will

explore the cellular processes regulated by Tgfbr2 that mediate the maintenance of these boundaries.

Acknowledgements

We would like to thank Ms. Anna Chytil and Dr. H. Moses for the kind gift of the Tgfbr2$^{LoxP/LoxP}$ mice. We thank Felecia Yu, Philip Hake, and Sirish Pulusani for excellent technical assistance. Dr. Serra is supported by NIH R01 AR46982 and R01 AR45605.

References

Baffi MO, Slattery E, Sohn P, Moses HL, Chytil A, Serra R. Conditional deletion of the TGF-beta type II receptor in Col2a expressing cells results in defects in the axial skeleton without alterations in chondrocyte differentiation or embryonic development of long bones. Dev Biol 2004;276:124–142. [PubMed: 15531369]

Bagnall KM, Sanders EJ. The binding pattern of peanut lectin associated with sclerotome migration and the formation of the vertebral axis in the chick embryo. Anat Embryol (Berl) 1989;180:505–513. [PubMed: 2619093]

Bagnall KM, Sanders EJ, Berdan RC. Communication compartments in the axial mesoderm of the chick embryo. Anat Embryol (Berl) 1992;186:195–204. [PubMed: 1510249]

Balling R, Helwig U, Nadeau J, Neubuser A, Schmahl W, Imai K. Pax genes and skeletal development. Ann N Y Acad Sci 1996;785:27–33. [PubMed: 8702151]

Bronner-Fraser M. Mechanisms of neural crest cell migration. BioEssays 1993;15:221–230. [PubMed: 8517851]

Bronner-Fraser M, Stern C. Effects of mesodermal tissues on avian neural crest cell migration. Dev Biol 1991;143:213–217. [PubMed: 1991548]

Bussen M, Petry M, Schuster-Gossler K, Leitges M, Gossler A, Kispert A. The T-box transcription factor Tbx18 maintains the separation of anterior and posterior somite compartments. Genes Dev 2004;18:1209–1221. [PubMed: 15155583]

Cancedda R, Cancedda FD, Castagnola P. Chondrocyte differentiation. Int Rev Cytol 1995;159:265–358. [PubMed: 7737795]

Christ B, Huang R, Wilting J. The development of the avian vertebral column. Anat Embryol (Berl) 2000;202:179–194. [PubMed: 10994991]

Christ B, Huang R, Scaal M. Formation and differentiation of the avian sclerotome. Anat Embryol (Berl) 2004;208:333–350. [PubMed: 15309628]

Chytil A, Magnuson MA, Wright CV, Moses HL. Conditional inactivation of the TGF-beta type II receptor using Cre:Lox. Genesis 2002;32:73–75. [PubMed: 11857781]

Dabovic B, Chen Y, Colarossi C, Obata H, Zambuto L, Perle MA, Rifkin DB. Bone abnormalities in latent TGF-[beta] binding protein (Ltbp)-3-null mice indicate a role for Ltbp-3 in modulating TGF-[beta] bioavailability. J Cell Biol 2002;156:227–232. [PubMed: 11790802]

Delise AM, Tuan RS. Analysis of N-cadherin function in limb mesenchymal chondrogenesis in vitro. Dev Dyn 2002;225:195–204. [PubMed: 12242719]

DeLise AM, Fischer L, Tuan RS. Cellular interactions and signaling in cartilage development. Osteoarthr Cartil 2000;8:309–334. [PubMed: 10966838]

Goldstein RS, Kalcheim C. Determination of epithelial half-somites in skeletal morphogenesis. Development 1992;116:441–445. [PubMed: 1286618]

Henderson DJ, Conway SJ, Copp AJ. Rib truncations and fusions in the Sp2H mouse reveal a role for Pax3 in specification of the ventro-lateral and posterior parts of the somite. Dev Biol 1999;209:143–158. [PubMed: 10208749]

Huang R, Zhi Q, Neubuser A, Muller TS, Brand-Saberi B, Christ B, Wilting J. Function of somite and somitocoele cells in the formation of the vertebral motion segment in avian embryos. Acta Anat (Basel) 1996;155:231–241. [PubMed: 8883534]

Huang R, Zhi Q, Brand-Saberi B, Christ B. New experimental evidence for somite resegmentation. Anat Embryol (Berl) 2000;202:195–200. [PubMed: 10994992]

Jaakkola E, Crane AM, Laiho K, Herzberg I, Sims AM, Bradbury L, Calin A, Brophy S, Kauppi M, Kaarela K, Wordsworth BP, Tuomilehto J, Brown MA. The effect of transforming growth factor beta1 gene polymorphisms in ankylosing spondylitis. Rheumatology (Oxford) 2004;43:32–38. [PubMed: 12890863]

Johnson J, Rhee J, Parsons SM, Brown D, Olson EN, Rawls A. The anterior/posterior polarity of somites is disrupted in paraxis-deficient mice. Dev Biol 2001;229:176–187. [PubMed: 11133162]

Kraus F, Haenig B, Kispert A. Cloning and expression analysis of the mouse T-box gene Tbx18. Mech Dev 2001;100:83–86. [PubMed: 11118889]

Leitges M, Neidhardt L, Haenig B, Herrmann BG, Kispert A. The paired homeobox gene Uncx4.1 specifies pedicles, transverse processes and proximal ribs of the vertebral column. Development 2000;127:2259–2267. [PubMed: 10804169]

Mansouri A, Voss AK, Thomas T, Yokota Y, Gruss P. Uncx4.1 is required for the formation of the pedicles and proximal ribs and acts upstream of Pax9. Development 2000;127:2251–2258. [PubMed: 10804168]

McGaughran JM, Oates A, Donnai D, Read AP, Tassabehji M. Mutations in PAX1 may be associated with Klippel-Feil syndrome. Eur J Hum Genet 2003;11:468–474. [PubMed: 12774041]

Mittapalli VR, Huang R, Patel K, Christ B, Scaal M. Arthrotome: a specific joint forming compartment in the avian somite. Dev Dyn 2005;234:48–53. [PubMed: 16028274]

Monsoro-Burq AH. Sclerotome development and morphogenesis: when experimental embryology meets genetics. Int J Dev Biol 2005;49:301–308. [PubMed: 15906245]

Monsoro-Burq AH, Bontoux M, Teillet MA, Le Douarin NM. Heterogeneity in the development of the vertebra. Proc Natl Acad Sci U S A 1994;91:10435–10439. [PubMed: 7937970]

Monsoro-Burq AH, Duprez D, Watanabe Y, Bontoux M, Vincent C, Brickell P, Le Douarin N. The role of bone morphogenetic proteins in vertebral development. Development 1996;122:3607–3616. [PubMed: 8951076]

Ovchinnikov DA, Deng JM, Ogunrinu G, Behringer RR. Col2a1-directed expression of Cre recombinase in differentiating chondrocytes in transgenic mice. Genesis 2000;26:145–146. [PubMed: 10686612]

Paavola LG, Wilson DB, Center EM. Histochemistry of the developing notochord, perichordal sheath and vertebrae in Danforth's short-tail (sd) and normal C57BL/6 mice. J Embryol Exp Morphol 1980;55:227–245. [PubMed: 7373196]

Pelton RW, Dickinson ME, Moses HL, Hogan BLM. In situ hybridization analysis of TGF-β 3 RNA expression during mouse development: comparative studies with TGF-b1 and -β 2. Development 1990;110:600–620.

Peters H, Doll U, Niessing J. Differential expression of the chicken Pax-1 and Pax-9 gene: in situ hybridization and immunohistochemical analysis. Dev Dyn 1995;203:1–16. [PubMed: 7647370]

Peters H, Wilm B, Sakai N, Imai K, Maas R, Balling R. Pax1 and Pax9 synergistically regulate vertebral column development. Development 1999;126:5399–5408. [PubMed: 10556064]

Poole AR. The histopathology of ankylosing spondylitis: are there unifying hypotheses? Am J Med Sci 1998;316:228–233. [PubMed: 9766483]

Rufai A, Benjamin M, Ralphs JR. The development of fibrocartilage in the rat intervertebral disc. Anat Embryol (Berl) 1995;192:53–62. [PubMed: 7486001]

Saga Y, Takeda H. The making of the somite: molecular events in vertebrate segmentation. Nat Rev, Genet 2001;2:835–845. [PubMed: 11715039]

Serra R, Johnson M, Filvaroff EH, LaBorde J, Sheehan DM, Derynck R, Moses HL. Expression of a truncated, kinase-defective TGF-β type II receptor in mouse skeletal tissue promotes terminal chondrocyte differentation and osteoarthritis. J Cell Biol 1997;139:541–552. [PubMed: 9334355]

Smits P, Lefebvre V. Sox5 and Sox6 are required for notochord extracellular matrix sheath formation, notochord cell survival and development of the nucleus pulposus of intervertebral discs. Development 2003;130:1135–1148. [PubMed: 12571105]

Sporle R, Schughart K. Paradox segmentation along inter- and intrasomitic borderlines is followed by dysmorphology of the axial skeleton in the open brain (opb) mouse mutant. Dev Genet 1998;22:359–373. [PubMed: 9664688]

Stern CD, Vasiliauskas D. Segmentation: a view from the border. Curr Top Dev Biol 2000;47:107–129. [PubMed: 10595303]

Stern CD, Sisodiya SM, Keynes RJ. Interactions between neurites and somite cells: inhibition and stimulation of nerve growth in the chick embryo. J Embryol Exp Morphol 1986;91:209–226. [PubMed: 3519826]

Stockdale FE, Nikovits W Jr, Christ B. Molecular and cellular biology of avian somite development. Dev Dyn 2000;219:304–321. [PubMed: 11066088]

Stringa E, Tuan RS. Chondrogenic cell subpopulation of chick embryonic calvarium: isolation by peanut agglutinin affinity chromatography and in vitro characterization. Anat Embryol (Berl) 1996;194:427–437. [PubMed: 8905010]

Tam PP, Trainor PA. Specification and segmentation of the paraxial mesoderm. Anat Embryol (Berl) 1994;189:275–305. [PubMed: 8074321]

Theiler K. Vertebral malformations. Adv Anat Embryol Cell Biol 1988;112:1–99. [PubMed: 3055848]

Tracy MR, Dormans JP, Kusumi K. Klippel-Feil syndrome: clinical features and current understanding of etiology. Clin Orthop Relat Res 2004:183–190. [PubMed: 15241163]

Walin J, Wilting J, Koseki H, Fritsch R, Christ B, Balling R. The role of Pax-1 in axial development. Development 1994;120:1109–1121. [PubMed: 8026324]

Wilkinson DG, Nieto MA. Detection of messenger RNA by in situ hybridization to tissue sections and whole mounts. Methods Enzymol 1993;225:361–373. [PubMed: 8231863]

Yamada Y, Okuizumi H, Miyauchi A, Takagi Y, Ikeda K, Harada A. Association of transforming growth factor beta1 genotype with spinal osteophytosis in Japanese women. Arthritis Rheum 2000;43:452–460. [PubMed: 10693888]

Yang X, Chen L, Xu X, Li C, Huang C, Deng CX. TGF-beta/Smad3 signals repress chondrocyte hypertrophic differentiation and are required for maintaining articular cartilage. J Cell Biol 2001;153:35–46. [PubMed: 11285272]

Zuscik MJ, Baden JF, Wu Q, Sheu TJ, Schwarz EM, Drissi H, O'Keefe RJ, Puzas JE, Rosier RN. 5-azacytidine alters TGF-beta and BMP signaling and induces maturation in articular chondrocytes. J Cell Biochem 2004;92:316–331. [PubMed: 15108358]

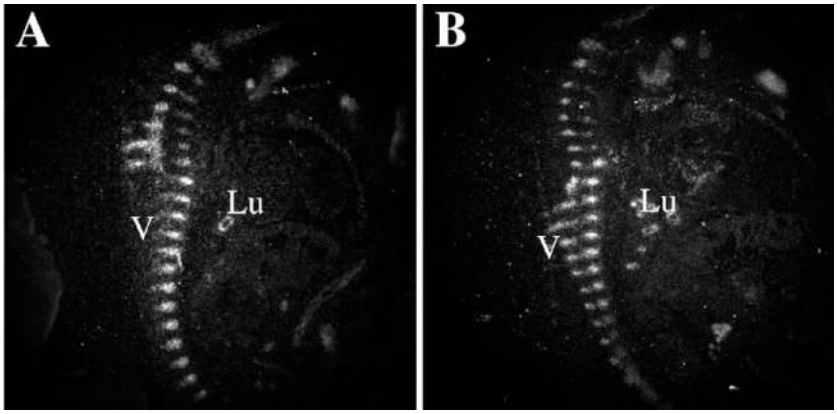

Fig. 1.

Effects of *Tgfbr2* deletion on Sox9 expression. Sagittal sections from control (A) and Col2acre$^{+/-}$;*Tgfbr*$^{loxP/loxP}$ (B) E12.5-day embryos were hybridized to an ^{35}S-labeled antisense Sox9 riboprobe. Sox 9 mRNA was detected by autoradiography and is seen as bright white grains on the dark field images shown. The developing vertebrae (V) and lung epithelium (Lu) were stained.

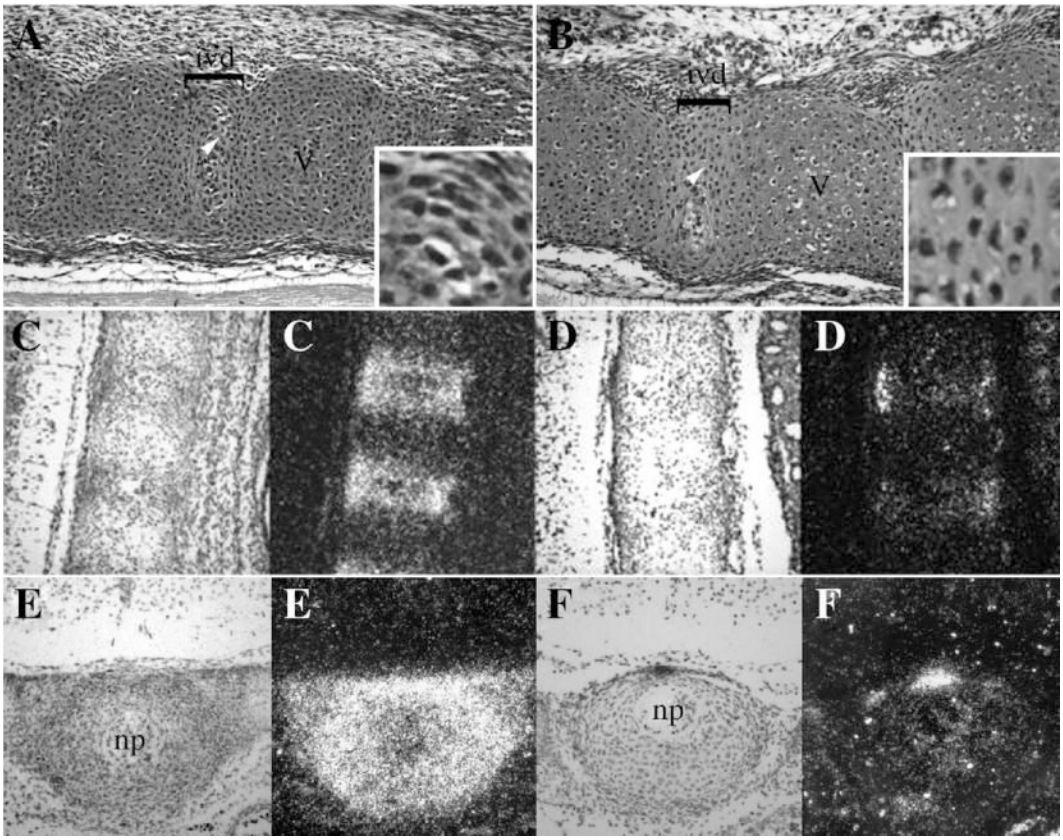

Fig. 2.

Effects of *Tgfbr2* deletion on the IVD. Sagittal sections from the upper thoracic region of E14.5-day control (A) and Col2acre$^{+/-}$;*Tgfbr*$^{loxP/loxP}$ (B) embryos were stained with H&E. In the control, the developing vertebrae (V) and intervertebral disc (ivd) were clearly demarcated (A). Cells in the annulus fibrosus of the IVD were spindle shaped in the controls (inset A). Cells in the annulus of Col2acre$^{+/-}$;*Tgfbr*$^{loxP/loxP}$ embryos had a round morphology (inset B). Ventral is to the top, dorsal to the bottom, rostral to the left, and caudal to the right in figures A and B. Fmod expression was determined by radioactive in situ hybridization to sagittal (C, D) and transverse (E, F) sections through the thoracic vertebrae of control (C, E) and Col2acre$^{+/-}$;*Tgfbr*$^{loxP/loxP}$ (D, F) mice. Transverse sections were taken through the area of the IVD as denoted by the nucleus pulposus (np). Both bright field (left) and dark field (right) images are shown. Areas of Fmod expression are seen as bright white grains in the darkfield images. Fmod expression is greatly reduced in Col2acre$^{+/-}$;*Tgfbr*$^{loxP/loxP}$ embryos.

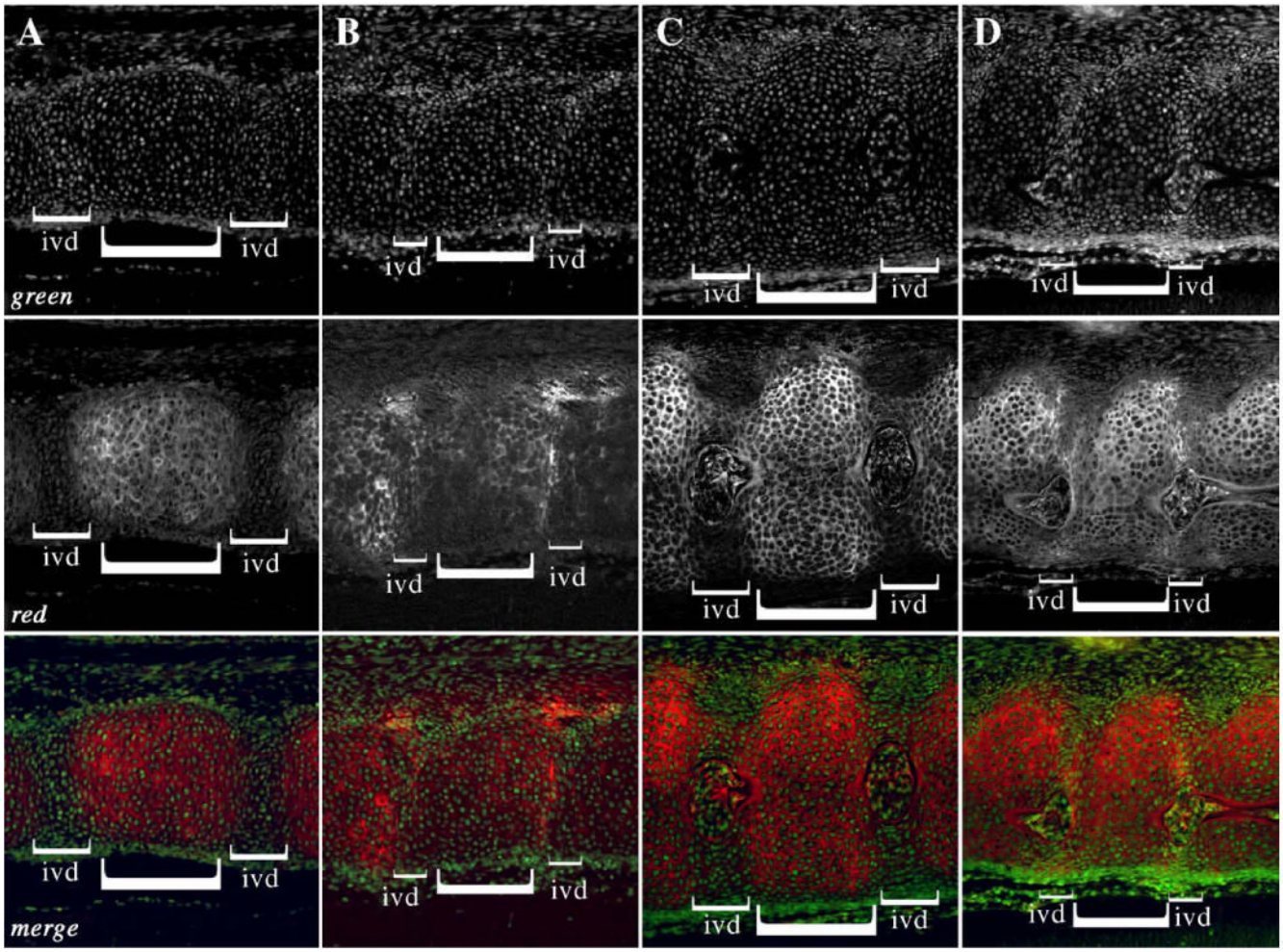

Fig. 3.

PNA staining in the E14.5 day axial skeleton. Sagittal sections from the thoracic (A, B) and cervical (C, D) regions of control (A, C) and Col2acre$^{+/-}$; *Tgfbr*$^{loxP/loxP}$ (B, D) E14.5-day embryos were stained with rhodamine conjugated PNA (red). The nuclei were counterstained with YoPro (green). The merged images are also shown. IVD and vertebrae are denoted with brackets. PNA staining is reduced or excluded from the IVD region in control embryos, whereas PNA stained cartilage is detected in the IVD region of Col2acre$^{+/-}$;*Tgfbr*$^{loxP/loxP}$ mice. Ventral is to the top, dorsal to the bottom, rostral to the left, and caudal to the right.

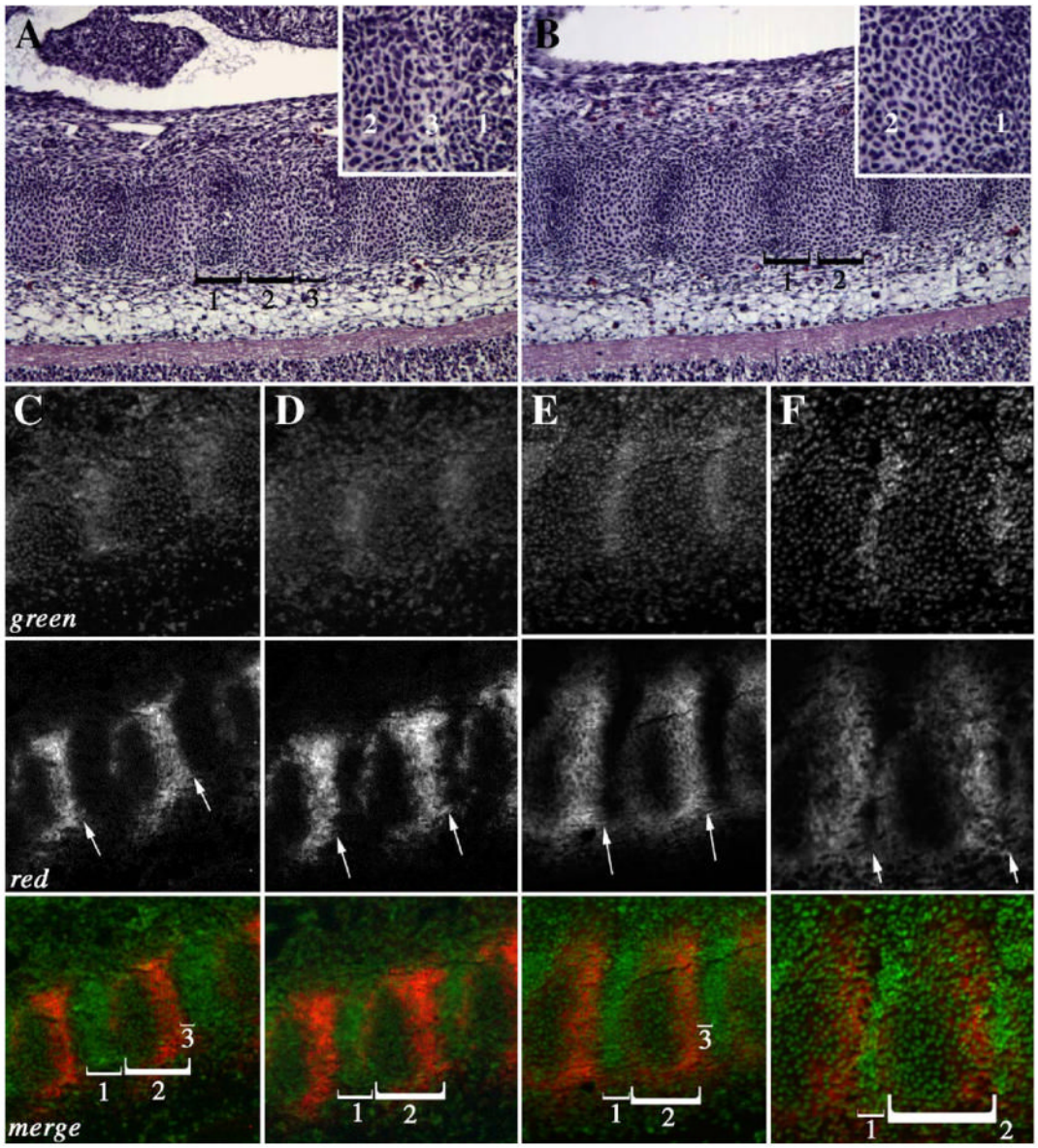

Fig. 4.

PNA staining in the E12.5 day axial skeleton. Sagittal sections from the thoracic (A–D) and cervical (E, F) regions of control (A, C, E) and Col2acre$^{+/-}$; *Tgfbr*$^{loxP/loxP}$ (B, D, F) E12.5-day embryos are shown. Subdomains of the sclerotome (brackets, 1–3) were observed in H&E stained sections of control (A) and Col2acre$^{+/-}$;*Tgfbr*$^{loxP/loxP}$ (B) embryos. Domain 3 was not observed in Col2acre$^{+/-}$;*Tgfbr*$^{loxP/loxP}$ mice (B). Insets show high magnification images of the area between domains 1 and 3 in control (A inset) and mutant (B inset) mice. (C–F) Sections were stained with rhodamine conjugated PNA (red; C–F). The nuclei were counterstained with YoPro (green). The merged images are also shown. A sharp boundary is observed at the caudal domain of PNA staining in control samples (arrows; C, E). The caudal boundary of PNA staining is blurred in Col2acre$^{+/-}$;*Tgfbr*$^{loxP/loxP}$ embryos (arrows D, F). Subdomains of the sclerotome (brackets, 1–3) were also defined by PNA staining. Domain 3, a dark area at the caudal end of the PNA staining domain in control mice (C, E merged), was not observed in

Col2acre$^{+/-}$; *Tgfbr*$^{loxP/loxP}$ mice (D, F merged). Ventral is to the top, dorsal to the bottom, rostral to the left, and caudal to the right.

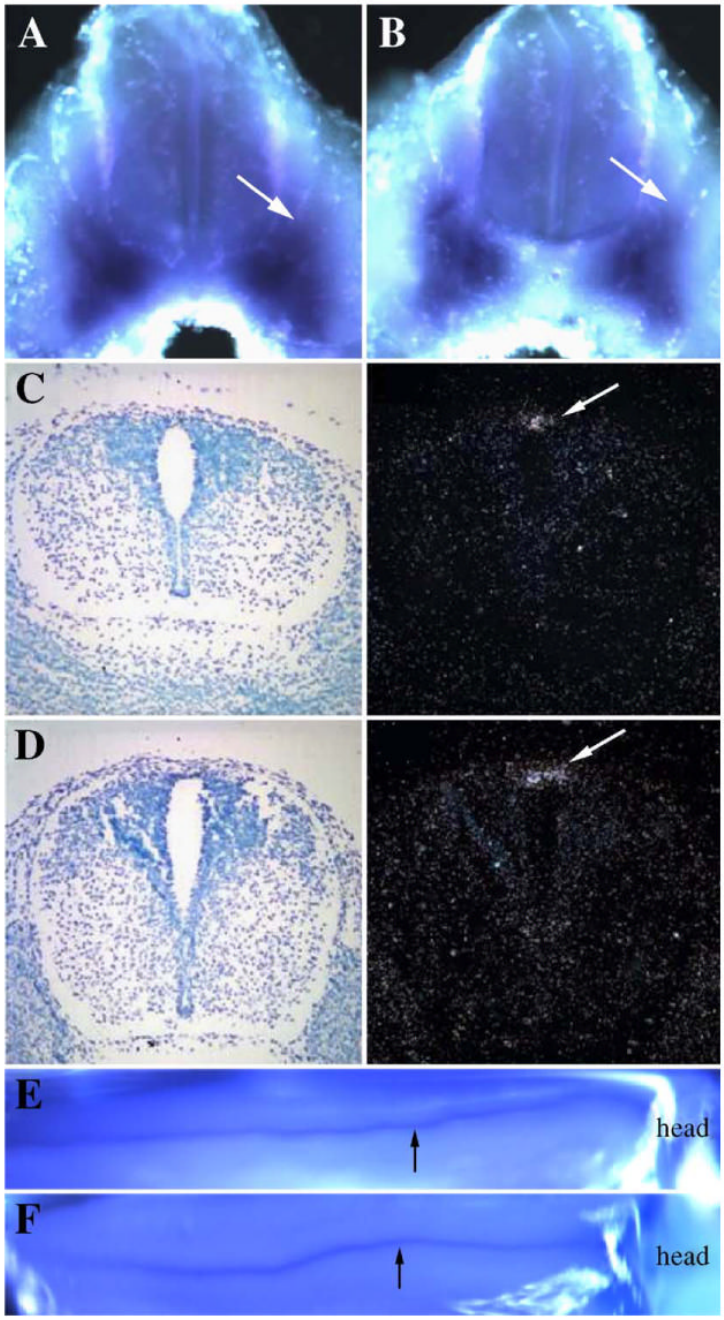

Fig. 5.

Role of *Tgfbr2* in dorsal–ventral patterning. The expression domains of Pax9 (A, B) and Msx1 (C–F) were determined in control (A, C, E) and Col2acre$^{+/-}$; *Tgfbr*$^{loxP/loxP}$ (B, D, F) E11.5day embryos by whole-mount (A, B, E, F) or E12.5-day embryos by radioactive in situ hybridization (C, D). Embryos were hybridized to digoxigenin labeled probes for whole-mount in situ hybridization and visualized using a colorimetric assay so that areas of expression are dark purple. Expression is seen as bright white grains on the dark field image for radioactive in situ hybridization. The expression domain of the ventral marker, Pax9, and dorsal marker, Msx1, were similar in control and Col2acre$^{+/-}$;*Tgfbr*$^{loxP/loxP}$ mice (arrows).

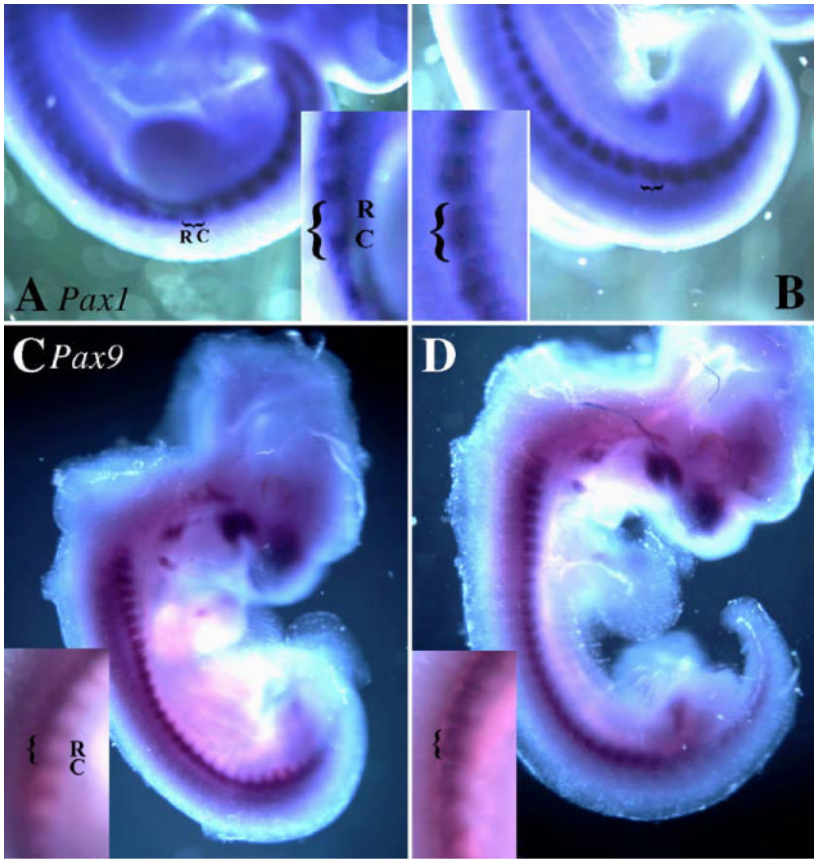

Fig. 6.

Effect of *Tgfbr2* deletion on the expression of caudal markers. The expression domains of Pax1 (A, B) and Pax 9 (C, D) were determined in control (A, C) and Col2acre$^{+/-}$;*Tgfbr*$^{loxP/loxP}$ (B, D) E11.5-day embryos by whole-mount in situ hybridization. Areas of expression are seen as dark purple staining. In control embryos, Pax1 and Pax9 mRNAs are preferentially expressed in the caudal domain of the sclerotome (A, C). Expression is expanded rostrally through the entire sclerotome in Col2acre$^{+/-}$;*Tgfbr*$^{loxP/loxP}$ embryos (B, D). Insets show a close-up of the region near the hindlimb.

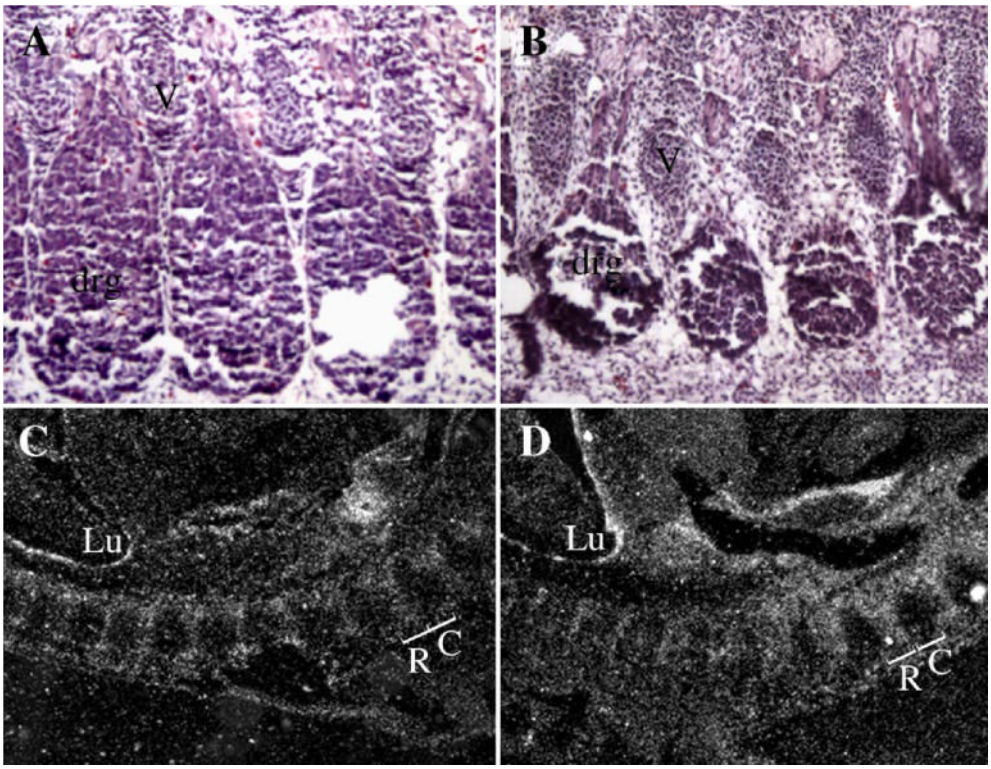

Fig. 7.

Effect of *Tgfbr2* deletion on the expression of rostral markers. Lateral sagittal sections from the thoracic region of E12.5-day control (A) and Col2acre$^{+/-}$; *Tgfbr*$^{loxP/loxP}$ (B) embryos were stained with H&E and the segmentation of the dorsal root ganglion (drg) in relation to the vertebrae (V) were examined. Drg was segmented properly in control and Col2acre$^{+/-}$;*Tgfbr*$^{loxP/loxP}$ embryos. The expression domain of Tbx18 (C, D) was determined in control (C) and Col2acre$^{+/-}$; *Tgfbr*$^{loxP/loxP}$ (D) at E12.5 day by radioactive in situ hybridization. Expression is seen as bright white grains in the dark field images. Tbx18 mRNA is restricted to the rostral domain of the sclerotome in both control and Col2acre$^{+/-}$;*Tgfbr*$^{loxP/loxP}$ embryos. An area near the hindlimb is shown. Rostral (R) and caudal (C) domains are indicated with brackets. Ventral is to the top, dorsal to the bottom, rostral to the left, and caudal to the right.

Table 1

Average percent labeled nuclei (standard deviation) and *T* test *P* value

Stage/Genotype	Cre−; *Tgfbr2*$^{+/lox}$	Cre+; *Tgfbr2*$^{lox/lox}$	*T* test
E14 cartilage*	16.4 (5.2)	17.8 (5.2)	*P* = 0.36
E12 cartilage**	13.4 (8.1)	14.4 (4.8)	*P* = 0.72
E12 sclerotome loose cells*	23.4 (5.1)	19.9 (4.7)	*P* = 0.02
E12 sclerotome condensed cells*	18.7 (8.2)	18.9 (7.5)	*P* = 0.46

* *n* = 4 embryos.

** *n* = 2 embryos.